Title: The SARS-CoV-2 Omicron BA.1 spike G446S potentiates HLA-A*24:02-restricted T cell immunity

Authors: Chihiro Motozono[1, 2*], Mako Toyoda[1], Toong Seng Tan[1], Hiroshi Hamana[3], Yoshiki Aritsu[4], Yusuke Miyashita[5, 6], Hiroyuki Oshiumi[5], Kimitoshi Nakamura[6], Seiji Okada[7], Keiko Udaka[8], Mizuki Kitamatsu[4], Hiroyuki Kishi[3], Takamasa Ueno[1*]

[1] Division of Infection and immunity, Joint Research Center for Human Retrovirus infection, Kumamoto University, Kumamoto 8600811, Japan
[2] Laboratory of Molecular Immunology, Immunology Frontier Research Center, Osaka University, Suita 5650871, Japan
[3] Department of Immunology, Faculty of Medicine, Academic Assembly, University of Toyama, Toyama 9300194, Japan
[4] Department of Applied Chemistry, Faculty of Science and Engineering, Kindai University, Osaka 577-8502, Japan
[5] Department of Immunology, Graduate School of Medical Sciences, Faculty of Life Sciences, Kumamoto University, Kumamoto 8608556, Japan
[6] Department of Pediatrics, Graduate School of Medical Sciences, Kumamoto University, Kumamoto 8608556, Japan
[7] Division of Hematopoiesis, Joint Research Center for Human Retrovirus Infection, Kumamoto University, Kumamoto 8600811, Japan
[8] Department of Immunology, Kochi University, Kochi 783-8505, Japan

***Correspondences:**
motozono@kumamoto-u.ac.jp (C.M.)
uenotaka@kumamoto-u.ac.jp (T.U.)

Conflict of interest: The authors declare that no competing interests exist.

Keywords: SARS-CoV-2; COVID-19; Omicron BA.1; Omicron BA.2; spike protein; T cells; TCR; franking region

Abstract (145/150 words)

Although the Omicron variant of the SARS-CoV-2 virus is resistant to neutralizing antibodies, it retains susceptibility to cellular immunity. Here, we characterized vaccine-induced T cells specific for various SARS-CoV-2 variants and identified HLA-A*24:02-restricted $CD8^+$ T cells that strongly suppressed Omicron BA.1 replication. Mutagenesis analyses revealed that a G446S mutation, located just outside the N-terminus of the cognate epitope, augmented TCR recognition of this variant. In contrast, no enhanced suppression of replication was observed against cells infected with the prototype, Omicron BA.2, and Delta variants that express G446. The enhancing effect of the G446S mutation was lost when target cells were treated with inhibitors of tripeptidyl peptidase II, a protein that mediates antigen processing. These results demonstrate that the G446S mutation in the Omicron BA.1 variant affects antigen processing/presentation and potentiates antiviral activity by vaccine-induced T cells, leading to enhanced T cell immunity towards emerging variants.

Introduction

Current mRNA vaccines against the severe acute respiratory syndrome coronavirus 2 (SARS-CoV-2) employ the viral spike protein as the target antigen. These vaccines elicit neutralizing antibodies and T-cell responses to the spike protein that play a central role in defending against viral infection and viral replication *in vivo*. The SARS-CoV-2 Omicron variant (BA.1; B.1.1.529.1), first identified in November 2021, is a novel variant that has rapidly spread around the globe. BA.1 has >30 mutations in the spike protein[1] that contribute to reduced sensitivity to vaccine-induced antibody neutralization[2, 3, 4, 5, 6]. In contrast, vaccine-induced SARS-CoV-2 specific T cells retain their reactivity to a number of different variants[7, 8]. Recent studies demonstrated that T cells induced in vaccinated donors can cross-recognize the Omicron variant[8, 9, 10, 11, 12]. However, the characteristics of vaccine-induced T cells cross-reactive for the Omicron virus are only poorly understood.

T cell epitopes are generated by the proteasome degradation of intracellular viral proteins into peptides that are subsequently trimmed by cytosolic aminopeptidases[13]. Some of these peptides are translocated via the transporter associated with antigen presentation (TAP) into the endoplasmic reticulum (ER) lumen and loaded onto HLA class I molecules. Peptide/HLA class I complexes are released from the ER and transported via the Golgi to the plasma membrane, where they are presented for recognition by $CD8^+$ T cells. Mutations within the peptide epitope directly affect HLA binding and T cell recognition. In addition, mutations outside the epitope can affect T cell recognition by interfering with the intracellular processing of virus-derived proteins[13, 14]. For example, a mutation from alanine to proline at HIV-1 Gag residue 146, immediately preceding the NH2 terminus of a dominant HLA-B57-restricted epitope, prevented NH2-terminal trimming of the optimal epitope by the endoplasmic reticulum aminopeptidase I[14]. These studies suggest that certain mutations located outside and nearby immunodominant epitopes may affect the T cell response to SARS-CoV-2 variants.

In this study, we demonstrated that a subset of vaccine-induced HLA-A*24:02-restricted T cells exhibited enhanced reactivity against the Omicron BA.1 variant. This enhanced reactivity was associated with a G446S mutation in the Omicron BA.1 spike protein that altered (enhanced) the processing and presentation of the associated antigenic peptide. Enhanced presentation of this epitope was also associated with greater inhibition of BA.1 replication by vaccine-induced T cells.

Results

Vaccine-induced immunodominant responses in the context of HLA-A*24:02

HLA-A*24:02 is one of the most widely distributed HLA-I alleles globally (predominantly in East Asia) [15]. A bioinformatic study identified three candidate HLA-A*24:02-binding peptides in the spike protein, RFDNPVLPF (RF9; residues 78-86), NYNYLYRLF (NF9; residues 448-456), and QYIKWPWYI (QI9; residues 1208-1216) [16]. All three peptides bound tightly to HLA-A*24:02 (**Table 1**). To investigate vaccine-induced immunodominant responses in the context of HLA-A*24:02, we obtained PBMCs from individuals that had been vaccinated with two doses of BNT162b2 or mRNA-1273 vaccines (n=29) (**Supplementary Table 1**). PBMC were stained with peptide/HLA tetramers of the three epitopes RF9/HLA-A*24:02 (RF9/A24), NF9/HLA-A*24:02 (NF9/A24), and QI9/HLA-A*24:02 (QI9/A24) (**Fig. 1a and Extended Data Fig. 1a**). NF9/A24- and QI9/A24-specific T cells were detected in 10 (34.5%) and 13 (44.8%), respectively, of 29 HLA-A*24:02$^+$ vaccinated donors (**Fig. 1b**). RF9/A24-specific T cells were detected in only 2 of 29 individuals (6.9%). These data indicate that CD8$^+$ T cells specific for NF9/A24 and QI9/A24 are predominantly induced in HLA-A*24:02$^+$ vaccinated donors.

To analyze the recognition of SARS-CoV-2 variants by NF9/A24- and QI9/A24-specific T cells, we stimulated PBMCs from ten donors (GV9, 15, 16, 26, 31, 33, 34, 36, 60, and 61) with the NF9 or QI9 peptides. After 14 days, proliferating T cells were evaluated for the upregulation of two activation markers, CD25 and CD137 (**Fig. 1c and Extended Data Fig. 1b**), as previously described [15, 17, 18]. The percentages of CD25$^+$CD137$^+$ T cells after stimulation with the NF9 peptide (median 3.5%) and QI9 peptide (median 4.5%) were significantly higher than those in the absence of the peptide (median <0.5%) (**Fig. 1d**, p = 0.0020 by Wilcoxon matched-pairs signed rank test; versus no peptide). There was no significant difference in the frequencies of NF9/A24 and QI9/A24-specific T cells (**Fig. 1d**, p = 0.6453 by Mann-Whitney test), consistent with the tetramer staining data (**Fig. 1b**). Taken together, our *ex vivo* and *in vitro* data indicate that NF9/A24 and QI9/A24 are immunodominant epitopes presented by HLA-A*24:02 in BNT162b2 or mRNA-1273 vaccinated donors.

Vaccine-induced NF9/A24-specific T cells efficiently recognize target cells expressing the Omicron BA.1 spike protein

To analyze the recognition of the prototype (D614G-bearing B.1 lineage), Omicron BA.1, and Delta (B.1.617.2) variants by vaccine-induced HLA-A*24:02-restricted T cells, we established T cell lines by stimulating of PBMCs from two HLA-A*24:02$^+$ vaccinated donors (GV34 and GV60) with the NF9 or QI9 peptides (**Extended Data Fig. 1c, d, e**). The resulting T cell lines were tested for the recognition of A549-

ACE2-A2402 cells (**Extended Data Fig. 1f**) that had been engineered to express spike protein from the prototype, Omicron BA.1 or Delta variants. These target cell lines expressed comparable levels of spike protein, as determined by western blot (**Extended Data Fig. 1g**). Interestingly, the level of IFN-γ production by the NF9-specific T cell lines from both donors was higher toward target cells expressing Omicron BA.1 spike protein and lower toward cells expressing Delta spike protein, compared to cells expressing the prototype spike protein (**Fig. 2a**). On the other hand, the level of IFN-γ production by the QI9-specific T cell lines was comparable against target cells expressing Omicron BA.1, Delta, and prototype spike proteins (**Fig. 2b**). The enhanced sensitivity of NF9/A24-specific T cells to Omicron BA.1 spike protein, compared to QI9/A24-specific T cells, was maintained at different E:T ratios (**Fig. 2c**). Analysis of a further six donors confirmed these results (**Fig. 2d**, $p < 0.0001$ by Mann-Whitney test versus prototype). Of note, diminished T cell sensitivity against target cells expressing the Delta spike protein is due to the presence of an L452R mutation in the NF9 peptide, a hallmark of the Delta spike protein (**Table 2**). These data extend our previous analysis of T cell recognition of target cells pulsed with the mutant peptide by T cells from COVID-19 convalescents[15] and vaccinated donors[18]. In contrast, there was no mutation within the NF9 epitope in Omicron BA.1 (**Table 2**), suggesting that Omicron BA.1 mutations of amino acid residues outside the NF9 peptide affect the sensitivity of the target cells to NF9/A24-specific T cells.

The G446S mutation in the SARS-CoV-2 Omicron BA.1 spike protein is responsible for enhanced NF9/A24-specific TCR recognition

We next identified TCR pairs specific for the NF9/A24 and QI9/A24 epitopes by single-cell sorting with NF9/A24 and QI9/A24 tetramers[19]. These studies focused on TCR sequences from 4 donors (**Supplementary Table 2**). Pairs of TCR α and β chains were reconstituted in a TCR-deficient NFAT-luciferase reporter cell line. TCRs specific for NF9/A24 (#5-3 and #12-3) and QI9/A24 (#43 and #57) were expressed on the cell surface and bound cognate tetramers at levels comparable to those of T cell lines (**Fig. 3a**). Both of the NF9/A24-specific TCR lines responded to cells expressing the Omicron BA.1 spike protein to a greater extent than those expressing the prototype, Alpha (B.1.1.7), Beta (B.1.351), and Gamma (P.1) spike proteins (**Fig. 3b**). These data indicate that the level of the NF9 peptide on the cell surface was enhanced in target cells expressing the Omicron BA.1 spike protein. Consistent with this, peptide-titration experiments using the #5-3 TCR indicated that the amount of NF9 peptide expressed on the target cells was almost 3-fold greater on cells expressing Omicron BA.1 spike protein than cells expressing the prototype

spike protein (**Extended Data Fig. 2a**). Also, the TCR responses were significantly reduced in cells expressing Delta and Lambda (C.37 lineage) spike protein, agreeing with our previous reports that L452R and L452Q in Delta and Lambda, respectively, mediate escape from vaccine-induced NF9/A24-specific T cells[18]. In contrast, both QI9/A24-specific TCRs responded comparably to cells expressing the spike protein from the prototype and variants (**Fig. 3b**).

It has been shown that mutations adjacent to T cell epitopes in HIV-1 can affect antigen processing and subsequent display to T cells [14, 20, 21, 22]. To determine whether this is also true for SARS-CoV-2 -specific T cells, we introduced mutations adjacent to the NF9 peptide sequence in BA.1 spike protein[1]. There are two mutations, N440K and G446S, located at 8 and 2 amino acids preceding the NF9 peptide sequence in Omicron BA.1 spike protein (**Table 2**). Therefore, we sought to examine whether N440K or G446S could enhance epitope recognition by NF9/A24-specific T cells.

The introduction of both mutations, or the G446S mutation alone, to the prototype spike protein, resulted in significantly enhanced recognition by NF9/A24-specific TCRs. In contrast, the introduction of N440K alone and reversion of the sequence (S446G) in Omicron BA.1 spike protein was recognized by NF9/A24-specific TCRs at levels similar to those induced by the prototype spike protein (**Fig. 3c**). Moreover, QI9/A24-specific TCRs comparably recognized all target cells tested, consistent with a comparable level of spike protein expression, as determined by western blot (**Extended Data Fig. 2b**). Taken together, our findings indicate that the N-terminal adjacent G446S mutation of the NF9 epitope in Omicron BA.1 spike protein is responsible for enhancing NF9/A24-specific TCR recognition.

Enhanced T cell recognition is diminished against Omicron BA.2 spike protein due to the lack of the G446S mutation.

The SARS-CoV-2 Omicron variant (B.1.1529) is comprised of three major lineages BA.1 (B.1.1529.1), BA.2 (B.1.1529.2), and BA.3 (B.1.1529.3)[1]. Following the initial spread of BA.1, BA.2 is now becoming the prevalent variant as of April 2022. Because the G446S mutation is lost in Omicron BA.2, we investigated the recognition of Omicron BA.2 by NF9-specific T cells. BA.2 spike protein-expressing cells were recognized by NF9/A24-specific TCRs to a lesser extent than those expressing BA.1 spike protein, and comparable to those expressing the prototype (**Fig. 3b**). Furthermore, NF9-specific T cells from eight vaccinated HLA-A*24:02^{+} donors exhibited decreased levels of IFN-γ in response to stimulation with target cells expressing Omicron BA.2 spike protein, similar to the levels elicited by the Omicron BA.1 reversion S446G (**Fig. 3d**, $p = 0.0002$ and $p = 0.0078$ by Mann-

Whitney test versus Omicron BA.2, Omicron BA.1/S446G, respectively). In contrast, QI9-specific T cells from the same donors produced comparable levels of IFN-γ in response to stimulation with target cells expressing all spike proteins tested (**Fig. 3d**). Together, these data suggest that the introduction of a serine at position 446 of Omicron BA.1 spike protein is sufficient to induce enhanced T cell recognition of the NF9 epitope. This enhanced recognition is diminished against Omicron BA.2 spike protein due to the absence of the G446S mutation.

Tripeptidyl peptidase II (TPPII) inhibitor reduces the enhanced recognition of the NF9 epitope

To determine how the G446S mutation affects the antigen processing pathway, we performed a TCR-sensitivity assay using Omicron BA.1 spike protein-expressing target cells pre-treated with a panel of protease inhibitors that are involved in N-terminal processing/trimming of the peptide; e.g., bestatin (aminopeptidase inhibitor), butabindide (tripeptidyl peptidase II inhibitor) and ERAP1 inhibitor compound 3[13]. The enhanced sensitivity of NF9/A24-specific TCRs to Omicron BA.1 spike by (GV34 #5-3, Vku19 #12-3, and GV34 #2-2) was significantly reduced in the presence of TPPII inhibitor (**Fig. 3e,** $p = 0.0456$ by Mann-Whitney test versus DMSO alone), although there was no difference in the sensitivity of QI9/A24-specific TCRs (GV34 #43, GV33 #57 and GV36 #10-2). These data suggest that TPPII might be one of the proteases involved in the efficient generation of the NF9 epitope.

NF9-specific T cells efficiently suppress the replication of Omicron BA.1, but not the BA.2, viral variants

We next investigated whether NF9-specific T cells have a superior capacity to suppress the replication of the Omicron BA.1 viral variant. A549 cells expressing ACE2/A2402 were infected with SARS-CoV-2 viral variants and cocultured with T cell lines specific for NF9/A24 and QI9/A24. Suppression of viral replication by T cells is evaluated by the amount of viral RNA in the supernatant at 72 h after infection. NF9/A24 and QI9/A24-specific T cells isolated from donor GV36, significantly inhibited replication of the prototype virus at 72 h (**Fig. 4a,** $p = 0.009$ and $p = 0.0036$ versus without T cells by unpaired two-tailed Student's t-test). NF9-specific T cells isolated from donors GV26, GV36, and GV60 also suppressed replication of Omicron BA.1 variant replication to a greater extent than the prototype or Omicron BA.2 (**Fig. 4b**). No suppression was observed against the Delta variant (**Fig. 4b**), presumably due to the T cell escape mutation L452R in the Delta spike protein (**Fig. 2c and 2d**). On the other hand, QI9-specific T cells comparably suppressed viral replication of prototype and these variants in all three donors tested (**Fig. 4c**). We

236 also tested the antiviral activity of T cells from three additional donors and confirmed
237 that NF9-specific T cells have the capacity to inhibit Omicron BA.1, but not BA.2
238 replication to a greater extent than the prototype. These data indicate that vaccine-
239 induced T cells can have an enhanced capacity to recognize and suppress emerging
240 SARS-CoV-2 BA.1 variant.
241

Discussion

In this study, we report that vaccine-induced HLA-A*24:02-restricted, NF9-specific T cells efficiently recognize target cells expressing the Omicron BA.1 spike protein and strongly suppress viral replication of the Omicron BA.1 variant compared to the prototype virus. The G446S mutation in Omicron BA.1 spike protein, located adjacent to the N terminus of the NF9 epitope (residues 448-456), is responsible for the efficient generation of the epitope. This is presumably due to enhanced antigen processing and presentation of the epitope. These data indicate that vaccine-induced T cells can have an enhanced capacity to cross recognize and suppress emerging SARS-CoV-2 variants.

The generation of HLA class I-restricted peptides is profoundly influenced by amino acid variations, not only within, but also around the core epitope. Changes in the epitope-flanking region can result in the inhibition of epitope presentation or a significant increase in the generation of the epitope[22]. In our study, we used a TCR-based quantification assay to demonstrate that the presentation of the NF9 epitope on the surface of Omicron BA.1 spike protein-expressing cells was estimated to be almost 3-fold increased relative to that of the prototype. The finding that T cell recognition of NF9 epitope was reduced when the Omicron BA.1 spike protein-expressing target cells were pre-treated with butabindide, an inhibitor of TPPII, suggested that generation of NF9 epitope requires TPPII-mediated removal of 2-3 amino acids from the N terminus of the peptide as TPPII is known to mediate this process[23]. This finding is consistent with reports that the flanking regions of some HIV-1 epitopes impact proteasomal processing of the epitope[14, 20]. Further studies are needed to clarify how mutations in the spike protein and other proteins in SARS-CoV-2 variants affect antigen processing/presentation for T cell recognition, providing better insights for the rational design of vaccine antigens to induce efficient cellular immunity.

We and others previously reported that the NF9 is an immunodominant epitope presented by HLA-A*24:02 both in convalescent[15, 24, 25, 26, 27, 28] and vaccinated donors[18]. However, the L452R and L452Q mutations in Delta/Epsilon and Lambda variants, respectively, conferred escape from NF9-specific T cell responses[15, 18]. In contrast, in this study, we demonstrated that NF9-specific T cells efficiently recognized target cells expressing Omicron BA.1 spike protein and suppressed viral replication of the Omicron BA.1 variant to a greater extent than that of the prototype. Interestingly, however, NF9-specific T cells only recognized and suppressed viral replication of the closely related variant Omicron BA.2 comparable to the prototype. This is presumably due to the absence of G446S mutation in BA.2 and prototype. It will be interesting to see whether vaccine-induced T cells respond

comparably, or differently, or control replication of SARS-CoV-2 variants of concern in the context of HLA-A*24:02 in vaccinated donors.

IFN-γ ELISpot or AIM (Activation-Induced marker) assays using overlapping peptides are powerful methods to evaluate the breadth of T cell responses to overall viral proteins in vaccinated and COVID-19 convalescent donors[29, 30]. Recent studies using these assays have demonstrated that T cells in vaccinated donors and convalescents can cross-recognize Omicron variants[8, 9, 11, 12]. However, these assays do not reveal antiviral functions of individual T cells against variants of concern, including the Omicron variant and the effect of mutations on antigen processing/presentation in virus-infected cells. Here, we found that a mutation located outside the epitope could enhance the antiviral activity of vaccine-induced T cells against the Omicron BA.1 variant. Thus, the antiviral assay for T cells demonstrated in this study will be tremendously useful for future vaccine development, and the combination of this quantitative assay with quantity assays by ELISpot assays would be important to access vaccine efficacy against variants.

296 **Author Contributions:**
297 C.M M.T T.S.T K.U performed the experiments.
298 Y.M K.N H.O S.O collected clinical samples.
299 H.H Y.A M.K H.K prepared reagents.
300 C.M M.T T.S.T T.U designed the experiments and interpreted the results.
301 C.M T.U wrote the original manuscript.
302 All authors reviewed and proofread the manuscript.
303
304 **Acknowledgments:**
305 We would like to thank all members of the Genotype to Phenotype Japan (G2P-
306 Japan) Consortium, especially Drs. Kei Sato (The University of Tokyo), Terumasa
307 Ikeda (Kumamoto University) for providing plasmids, reagents, and cells, and Dr.
308 Kazuhisa Yoshimura (Tokyo Metropolitan Institute of Public Health) and Drs.
309 Tomohiko Takasaki and Jun-Ichi Sakuragi (Kanagawa Prefectural Institute of Public
310 Health) for providing viruses. We thank Dr. Masafumi Takiguchi (Kumamoto
311 University) for providing C1R-A2402 cells. We thank Dr. David L. Woodland for
312 assistance in editing the manuscript. This study was supported in part by AMED
313 Research Program on Emerging and Re-emerging Infectious Diseases
314 20fk0108539h0001 (to T.U.) and 20fk0108451s0101 (to T.U.) and AMED Research
315 Program on HIV/AIDS 21fk0410046 (to C.M.), JSPS KAKENHI Grant-in-Aid for
316 Scientific Research B 19H03703, 22H03119 (to T.U.) and 22H02877 (to C.M.),
317 Scientific Research C 19K07623 (to C.M.) and 22K07089 (to M.T.), Takeda Science
318 Foundation (to C.M. and M.T) and an intramural grant from Kumamoto University
319 COVID-19 Research Projects (AMABIE) (to C.M.), IMAI MEMORIAL TRUST FOR
320 AIDS RESERARCH (to M.T.), Shin-Nihon Foundation of Advanced Medical
321 Research (to M.T.).
322
323

References

1. Viana, R. *et al.* Rapid epidemic expansion of the SARS-CoV-2 Omicron variant in southern Africa. *Nature* (2022).
2. Cele, S. *et al.* Omicron extensively but incompletely escapes Pfizer BNT162b2 neutralization. *Nature* (2021).
3. Cameroni, E. *et al.* Broadly neutralizing antibodies overcome SARS-CoV-2 Omicron antigenic shift. *Nature* (2021).
4. Cao, Y. *et al.* Omicron escapes the majority of existing SARS-CoV-2 neutralizing antibodies. *Nature* (2021).
5. Planas, D. *et al.* Considerable escape of SARS-CoV-2 Omicron to antibody neutralization. *Nature* (2021).
6. Meng, B. *et al.* Altered TMPRSS2 usage by SARS-CoV-2 Omicron impacts tropism and fusogenicity. *Nature* (2022).
7. Tarke, A. *et al.* Impact of SARS-CoV-2 variants on the total CD4(+) and CD8(+) T cell reactivity in infected or vaccinated individuals. *Cell Rep Med* **2**, 100355 (2021).
8. Tarke, A. *et al.* SARS-CoV-2 vaccination induces immunological T cell memory able to cross-recognize variants from Alpha to Omicron. *Cell* (2022).
9. Keeton, R. *et al.* T cell responses to SARS-CoV-2 spike cross-recognize Omicron. *Nature* (2022).
10. GeurtsvanKessel, C.H. *et al.* Divergent SARS CoV-2 Omicron-reactive T- and B cell responses in COVID-19 vaccine recipients. *Sci Immunol*, eabo2202 (2022).
11. Gao, Y. *et al.* Ancestral SARS-CoV-2-specific T cells cross-recognize the Omicron variant. *Nat Med* (2022).
12. Naranbhai, V. *et al.* T cell reactivity to the SARS-CoV-2 Omicron variant is preserved in most but not all individuals. *Cell* **185**, 1041-1051 e1046 (2022).
13. Neefjes, J., Jongsma, M.L., Paul, P. & Bakke, O. Towards a systems understanding of MHC class I and MHC class II antigen presentation. *Nat Rev Immunol* **11**, 823-836 (2011).
14. Draenert, R. *et al.* Immune selection for altered antigen processing leads to cytotoxic T lymphocyte escape in chronic HIV-1 infection. *J Exp Med* **199**, 905-915 (2004).
15. Motozono, C. *et al.* SARS-CoV-2 spike L452R variant evades cellular immunity and increases infectivity. *Cell Host Microbe* **29**, 1124-1136 (2021).
16. Kiyotani, K., Toyoshima, Y., Nemoto, K. & Nakamura, Y. Bioinformatic prediction of potential T cell epitopes for SARS-Cov-2. *J Hum Genet* **65**, 569-575 (2020).

17. Wolfl, M. *et al.* Activation-induced expression of CD137 permits detection, isolation, and expansion of the full repertoire of $CD8^+$ T cells responding to antigen without requiring knowledge of epitope specificities. *Blood* **110**, 201-210 (2007).
18. Kimura, I. *et al.* The SARS-CoV-2 Lambda variant exhibits enhanced infectivity and immune resistance. *Cell Rep* **38**, 110218 (2022).
19. Hamana, H., Shitaoka, K., Kishi, H., Ozawa, T. & Muraguchi, A. A novel, rapid and efficient method of cloning functional antigen-specific T-cell receptors from single human and mouse T-cells. *Biochem Biophys Res Commun* **474**, 709-714 (2016).
20. Milicic, A. *et al.* CD8+ T cell epitope-flanking mutations disrupt proteasomal processing of HIV-1 Nef. *J Immunol* **175**, 4618-4626 (2005).
21. Le Gall, S., Stamegna, P. & Walker, B.D. Portable flanking sequences modulate CTL epitope processing. *J Clin Invest* **117**, 3563-3575 (2007).
22. Del Val, M., Schlicht, H.J., Ruppert, T., Reddehase, M.J. & Koszinowski, U.H. Efficient processing of an antigenic sequence for presentation by MHC class I molecules depends on its neighboring residues in the protein. *Cell* **66**, 1145-1153 (1991).
23. Tomkinson, B. Tripeptidyl peptidases: enzymes that count. *Trends Biochem Sci* **24**, 355-359 (1999).
24. Gao, A. *et al.* Learning from HIV-1 to predict the immunogenicity of T cell epitopes in SARS-COV-2. *iScience*, 102311 (2021).
25. Hu, C. *et al.* Identification of Cross-Reactive CD8(+) T Cell Receptors with High Functional Avidity to a SARS-CoV-2 Immunodominant Epitope and Its Natural Mutant Variants. *Genes Dis* (2021).
26. Kared, H. *et al.* SARS-CoV-2-specific $CD8^+$ T cell responses in convalescent COVID-19 individuals. *J Clin Invest* **131** (2021).
27. Rowntree, L.C. *et al.* SARS-CoV-2-specific CD8(+) T-cell responses and TCR signatures in the context of a prominent HLA-A*24:02 allomorph. *Immunol Cell Biol* (2021).
28. Zhang, H. *et al.* Profiling CD8(+) T cell epitopes of COVID-19 convalescents reveals reduced cellular immune responses to SARS-CoV-2 variants. *Cell Rep* **36**, 109708 (2021).
29. Grifoni, A. *et al.* Targets of T Cell Responses to SARS-CoV-2 Coronavirus in Humans with COVID-19 Disease and Unexposed Individuals. *Cell* **181**, 1489-1501 e1415 (2020).
30. Peng, Y. *et al.* Broad and strong memory CD4(+) and CD8(+) T cells induced by SARS-CoV-2 in UK convalescent individuals following COVID-19. *Nat*

Immunol **21**, 1336-1345 (2020).

31. Karaki, S. *et al.* HLA-B51 transgenic mice as recipients for production of polymorphic HLA-A, B-specific antibodies. *Immunogenetics* **37**, 139-142 (1993).
32. Mashiba, T. *et al.* Identification of CTL epitopes in hepatitis C virus by a genome-wide computational scanning and a rational design of peptide vaccine. *Immunogenetics* **59**, 197-209 (2007).
33. Dolton, G. *et al.* More tricks with tetramers: a practical guide to staining T cells with peptide-MHC multimers. *Immunology* **146**, 11-22 (2015).
34. Suzuki, R. *et al.* Attenuated fusogenicity and pathogenicity of SARS-CoV-2 Omicron variant. *Nature* **603**, 700-705 (2022).
35. Yamasoba, D. *et al.* Virological characteristics of SARS-CoV-2 BA.2 variant. *bioRxiv*, 2022.2002.2014.480335 (2022).
36. Tan, T.S., Toyoda, M., Tokunaga, K. & Ueno, T. Aromatic Side Chain at Position 412 of SERINC5 Exerts Restriction Activity toward HIV-1 and Other Retroviruses. *J Virol* **95**, e0063421 (2021).
37. Miyama, T. *et al.* Highly functional T-cell receptor repertoires are abundant in stem memory T cells and highly shared among individuals. *Sci Rep* **7**, 3663 (2017).
38. Giudicelli, V., Brochet, X. & Lefranc, M.P. IMGT/V-QUEST: IMGT standardized analysis of the immunoglobulin (IG) and T cell receptor (TR) nucleotide sequences. *Cold Spring Harb Protoc* **2011**, 695-715 (2011).

Figure legends

Fig. 1 | Detection of HLA-A*24:02-restricted antigen-specific T cells in vaccinated donors.

(**a and b**) Detection of HLA-A*24:02-restricted antigen-specific T cells in PBMCs by HLA tetramers. **a**, Representative FACS plots showing tetramer$^+$ CD8$^+$ T cells of an HLA-A24-negative vaccinated donor, GV17 (upper), and an HLA-A24-positive vaccinated donor, GV16 (lower). See also **Extended Data Fig. 1a** (Gating strategy). **b,** The median of the percentage of RF9/A24, NF9/A24, and QI9/A24 tetramer$^+$CD8$^+$ T cells. **c and d**, Detection of HLA-A*24:02-restricted antigen-specific T cell lines *in vitro*. **c,** Representative FACS plots showing surface expression of CD25 and CD137 on the CD8$^+$ T cell subset of a vaccinated donor, GV60. See also **Extended Data Fig. 1b** (Gating strategy). **d,** The median of the percentage of CD25$^+$CD137$^+$ cells among CD8$^+$ T cells. See also **Supplementary Table 1** (donor information). In **a and c**, the numbers in the FACS plot represent the percentage of gated cells among CD8$^+$ T cells. In **b**, the median of % tetramer$^+$ population in HLA-A24 negative donors was <0.05%. HLA-A24$^+$ donors showing a >0.1% tetramer$^+$ response were considered to be responders. In **d**, a statistically significant difference versus value without peptide (*p < 0.05) is determined by Wilcoxon matched-pairs signed rank, and versus peptide is determined by Mann-Whitney test. ns, no statistical significance.

Fig. 2 | T cell recognition to target cells expressing variant spike protein.

(**a and b**) HLA-A24-positive T cell lines of vaccinated donors were stimulated with A549-ACE/A2402 (**Extended Data Fig. 1f**) expressing spike protein derived from prototype, Omicron, and Delta variants. Representative FACS plots showing intracellular expression of IFN-γ in the NF9-specific CD8$^+$ T cells (**a**) and QI9-specific CD8$^+$ T cells (**b**) in two vaccinated donors (GV34 and GV60). **c**, The level of IFN-γ production of NF9- and QI9-specific T cells in response to spike-expressing target cells in two vaccinated donors, GV34 (upper) and GV60 (lower). Data represent the mean of triplicates. **d**, Fold changes in IFN-γ expression by NF9-specific T cells (left) and QI9-specific T cells (right) compared to the target cells expressing prototype spike in eight vaccinated donors (GV15, 26, 31, 33, 34, 36, 60, and 61) are shown. In **a** and **b**, the numbers in the FACS plot represent the percentage of IFN-γ$^+$ cells among CD8$^+$ T cells. In **d**, a statistically significant difference versus prototype spike (*p < 0.05) is determined by a Mann-Whitney test. ns, no statistical significance.

Fig. 3 | Identification of mutation associated with increased TCR sensitivity.

TCR-peptide/HLA interaction on a TCR-transduced Jurkat NFAT-luciferase reporter cell. **a**, Jurkat cells alone (shaded histogram) or those expressing NF9/A24-specific TCRs (#5-3 and #12-3) or QI9/A24-specific TCRs (#43 and #57) (open histogram) were stained with anti-CD3 mAb and their cognate HLA-A24 tetramers and then analyzed by flow cytometry. **b and c**, the level of peptide/HLA complexes was evaluated by NFAT-luciferase reporter activity of TCR-transduced Jurkat cells. Data of NF9/A24-specific TCRs (**b**) and QI9/A24-specific TCRs (**c**) are shown. Fold changes of reporter activity by NF9/A24- and QI9/A24-specific TCRs compared to the target cells expressing prototype spike protein are shown. (**d**) Fold changes of IFN-γ by NF9-specific T cells (left) and QI9-specific T cells (right) compared to the target cells expressing Omicron BA.1 spike protein in eight vaccinated donors (GV15, 26, 31, 33, 34, 36, 60 and 61) are shown. A statistically significant difference versus Omicron BA.1 spike (*$p < 0.05$) is determined Mann-Whitney test. ns, no statistical significance. (**e**) The level of peptide/HLA complexes is evaluated following treatment with inhibitors, bestatin (120 μM), butabindide (150 μM), and ERAP1 inhibitor (50 μM). The effect of inhibitors was evaluated as reporter activity and shown by fold change of the level of peptide/HLA on target cells expressing Omicron BA.1 reversion S446G spike protein. Statistical analysis versus DMSO alone was determined by Mann-Whitney test. **b, c** Statistical analysis versus parental was done by unpaired two-tailed Student's t-test. ns, no statistical significance. **b, c** Data are expressed as mean ± SD. **d, e** Data are expressed as a median. **b, c, e** Data are representative of three independent experiments.

Fig. 4 | Inhibition of SARS-CoV-2 viral replication by HLA-A24-restricted T cell lines from vaccinated donors.

(**a**) Viral replication of the prototype in the presence of NF9- or QI9-specific T cells from GV36, or without T cells. **b and c**, Inhibition of viral replication by NF9-specific T cells (**b**) and QI9-specific T cells (**c**) compared to without T cells in three vaccinated donors are shown. In **a**, a statistically significant difference versus without T cells (*$p < 0.05$) was determined by an unpaired two-tailed Student's t-test. In **b** and **c**, a statistically significant difference versus prototype (*$p < 0.05$) was determined by a Mann-Whitney test. ns, no statistical significance. **a-c** Data are representative of two independent experiments.

Table 1 Binding of spike-derived epitopes to HLA-A*24:02

Table 2 Spike-derived HLA-A24-restricted NF9 epitopes and the N-terminal flanking region from the variant

499

Extended Data Fig. 1. Gating strategy and T cell and cell lines used in this study (**a-c**) Flow cytometry gating strategy of tetramer staining in PBMCs from donor GV16 (**a**), $CD25^{+}CD137^{+}$ activated T cell lines from donor GV60 (**b**) and tetramer staining of T cell lines from GV60 (**c**). (**d**) NF9 and QI9 stimulated-T cell lines used in this study. (**e**) IFN-γ production in peptide titration of the NF9 and QI9 peptide in T cell lines from GV34 and GV60 donors. (**f**) GFP expression of A549-ACE2-A2402-IRES-GFP cells. A549-ACE2 parental (shaded histogram) and FACS-sorted A549-ACE2-A2402-IRES-GFP cells (open histogram) are shown. (**g**) Western blot. Representative blots of cells expressing prototype, Omicron BA.1, and Delta spike (S) protein.

Extended Data Fig. 2. (**a**) TCR sensitivity of GV34 #5-3 toward cells expressing spike protein and peptide-pulsed target cells. (**b**) Representative western blots of cells expressing various spike (S) proteins.

Supplementary Table 1. Human PBMCs used in this study, related to Fig. 1.

Supplementary Table 2. TCR sequences isolated from NF9/A24- and QI9/A24-specific T cells by single-cell analysis, related to Fig. 3.

Supplementary Table 3. Primers for the construction of spike derivatives, related to Fig. 3.

Methods

Ethics Statement

For the use of human specimens, all protocols involving human subjects recruited at Kumamoto University were reviewed and approved by the Institutional Review Boards of Kumamoto University (approval numbers 2074 and 477). All human subjects provided written informed consent.

Collection of human PBMCs

Human PBMCs were obtained from thirty HLA-A*24:02-positive BNT162b2 or mRNA-1273 vaccinated donors (median age: 24, range: 18-79, 67% male), five HLA-A*24:02-negative BNT162b2-vaccinated donors (median age: 24, range: 18-28, 60% Female) (**Supplementary Table 1**). PBMCs were purified by a density gradient centrifugation using Ficoll-Paque Plus (GE Healthcare Life Sciences, Cat# 17-1440-03) and stored in liquid nitrogen until further use.

Cell Culture

A549-ACE2/A2402 cells, the A549 cells stably expressing human ACE2 and HLA-A*24:02-IRES-GFP, were generated by retroviral transduction as previously described[15, 19] and were maintained in Ham's-F12 (Wako, Cat# 080-08565) containing 10% fetal bovine serum (FBS). C1R cells expressing HLA-A*24:02 (C1R-A2402) [31] and TCR-deficient Jurkat cells expressing luciferase gene (JurkatΔ-Luc) were maintained in RPMI 1640 medium (Thermo Fisher Scientific, Cat# 11875101) containing 10% FBS.

Virus

Four clinically isolated SARS-CoV-2 lineages were used: SARS-CoV-2 Wuhan strain [SARS-CoV-2/Hu/DP/Kng/19-020 (DDBJ Accession ID: LC528232)], was provided from Kanagawa Prefectural Institute of Public Health. A B.1.617.2 (Delta) lineage [hCoV 19/Japan/TKYK01734/2021 (GISAID Accession ID: EPI_ISL_2080609)], and a B.1.1.529 (Omicron/BA.1) lineage [hCoV hCoV-19/Japan/TKYX00012/2021 (GISAID Accession ID: EPI_ISL_8559478)] were provided from Tokyo Metropolitan Institute of Public Health, Tokyo, Japan. B.1.1.529 (Omicron/BA.2) lineage [hCoV hCoV-19/Japan/TY40-385-P1/2022 (GISAID Accession ID: EPI_ISL_9595859)] were provided from National Institute of Infectious Diseases, Tokyo, Japan.

The peptide-dependent stabilization assay

The HLA binding of peptide was analyzed as previously described[32]. Briefly, TAP-deficient C1R-A24 cells were incubated at 26 °C overnight. A total of 1×10^5 cells was incubated with 1 μM β2-microglobulin (β2m) and graded concentrations of peptides in 96-well U-bottom plates. Cells were incubated at 26 °C for 1 h and then at 37 °C for 4 h. At the end of the incubation, unbound peptides were removed, and cells were stained with twice the saturating concentration of the first antibodies. After staining with FITC-labeled F(ab')2 goat anti-mouse IgG (Leinco), cells were analyzed by FACScan (BD, San Jose, CA, USA). The mean fluorescence intensity (MFI) was calculated with Cell QuestTM, and the mean values of duplicates were presented. Peptide binding is normalized by high-binder peptide (TYLPTNASL) and low-binder peptide (RVWESATPL) in each experiment.

Tetramer staining

SARS-CoV-2-derived peptides-loaded MHC class I (pMHCI) tetramers were generated by QuickSwitch™ Quant HLA-A*24:02 Tetramer Kit-PE (MBL International Corporation, Cat# TB-7302-K1) according to the manufacturer's protocol. The rate of peptide exchange was quantitated by flow cytometry, and the tetramers, at a rate of more than 90%, were used for staining PBMCs as previously described[33]. After treatment with a protein kinase inhibitor, Dasatinib (Cat# A10290-25, AdooQ) for 30 min at 37°C, PBMCs were stained with tetramers for 30 min on ice. After tetramer staining, cells were counterstained with anti-PE unconjugated mAb (Cat# 408104, Biolegend) for 20 min on ice and surface stained with the following antibodies: CD3 BV421 (UCHT1), CD8 APCcy7 (RPA-T8), CD14 PerCP/Cy5.5 (HCD14), CD19 PerCP/Cy5.5 (HIB19; Biolegend) was performed. Dead cells were stained with 7-aminoactinomycin D (Biolegend, Cat# 420404). After incubation for 20 min on ice, the cells were fixed with 1% paraformaldehyde (Nacalai Tesque, Cat# 09154-85), and the levels of tetramer$^+$CD8$^+$ T cells were analyzed by flow cytometry using a FACS Canto II (BD Biosciences). The data obtained by flow cytometry were analyzed with FlowJo software (Tree Star).

Activation-Induced Marker Assay

An activation-induced marker assay was performed as previously described[15, 17]. Briefly, human PBMCs were pulsed with 100 nM of the NF9 peptide (NYNYLYRLF, residues 448-456 of the SARS-CoV-2 spike protein) and the QI9 peptide (QYIKWPWYI, residues 1208-1216 of the SARS-CoV-2 spike protein) maintained in RPMI 1640 medium (Thermo Fisher Scientific, Cat# 11875101) containing 10% FBS and 30 U/ml recombinant human IL-2 (Peprotec, Cat# 200-02) for 14 days. The *in-vitro* expanded CD8$^+$ T cells (i.e., T cell lines) were restimulated with or without the

peptide. After incubation at 37°C for 24 h, the cells were washed, and surface stained with following antibodies: CD3 FITC (UCHT1), CD8 APCcy7 (RPA-T8), CD14 PerCP/Cy5.5 (HCD14), CD19 PerCP/Cy5.5 (HIB19), CD25 PEcy7 (M-A251) and CD137 APC (4B4-1; Biolegend). Dead cells were stained with 7-aminoactinomycin D (Biolegend, Cat# 420404). After incubation for 20 min on ice, the cells were fixed with 1% paraformaldehyde (Nacalai Tesque, Cat# 09154-85), and the levels of protein surface expression were analyzed by flow cytometry using a FACS Canto II (BD Biosciences). The data obtained by flow cytometry were analyzed with FlowJo software (Tree Star).

Plasmid Construction

Plasmids expressing the SARS-CoV-2 spike proteins of the parental (D614G-bearing B.1 lineage), Alpha (B.1.1.7), Beta (B.1.351), Gamma (P.1), Lambda (C.37 lineage) and Delta (B.1.617.2), Omicron BA.1 (B.1.1529.1), and Omicron BA.2 (B.1.1529.2) variant were prepared in our previous studies[18, 34, 35]. Plasmids expressing the point mutants were generated by site-directed overlap extension PCR using pC-SARS2-spike D614G or SARS2-Omicron-spike as the template and the following primers listed in **Supplementary Table 3.** Primers for the construction of spike derivatives, related to Fig. 2 and 3. The resulting PCR fragment was digested with KpnI and NotI and inserted into the corresponding site of the pCAGGS vector. Nucleotide sequences were determined by Genetic Analyzer 3500xL (Applied Biosystems) and the sequence data were analyzed by GENETYX v12 (GENETYX Corporation).

Intracellular Cytokine Staining

Intracellular cytokine staining was performed as previously described[15]. Briefly, A549-ACE2-A2402 cells (3×10^5 cells) were transfected with 2 μg of plasmids expressing prototype spike or its derivatives using PEI Max (Polysciences, Cat# 24765-1) according to the manufacturer's protocol. At two days post transfection, the transfectants were harvested and mixed with the T cell lines generated from HLA-A*24:02$^+$ vaccinated donors (see above) and incubated with RPMI 1640 medium (Thermo Fisher Scientific, Cat# 11875101) containing 10% FBS, 5 μg/ml brefeldin A (Sigma-Aldrich, Cat# B7651) in a 96-well U plate at 37°C for 5 h. The cells were washed, and surface stained with following antibodies: CD3 FITC (UCHT1), CD8 APCcy7 (RPA-T8), CD14 PerCP/Cy5.5 (HCD14), CD19 PerCP/Cy5.5 (HIB19; Biolegend). Dead cells were stained with 7-aminoactinomycin D (Biolegend, Cat# 420404). After incubation at 4°C for 20 min, the cells were fixed and permeabilized with a Cytofix/Cytoperm Fixation/Permeabilization solution kit (BD Biosciences, Cat#

554714) and were stained with IFN-γ PE (4S.B3; BD). After incubation at room temperature for 30 min, the cells were washed, and levels of protein expression were analyzed by flow cytometry using a FACS Canto II (BD Biosciences) followed by analysis using FlowJo software (Tree Star).

Western blotting

The samples for immunoblotting were prepared as described previously[36] with some modifications. Briefly, transfected cells were lysed on ice for 15 min in a buffer (100 mM NaCl, 1 mM TCEP [Tris (2-carboxyethyl) phosphine hydrochloride], 2X protease inhibitor, and 10 mM HEPES; pH 7.5) containing 1% n-dodecyl-b-D-maltoside (DDM; Thermo Scientific). The resultant samples were resuspended in 1X Laemmli buffer containing 5% β-Mercaptoethanol (Bio-Rad), boiled for 10 min and subjected to protein separation by SDS-PAGE in 4 – 20% Mini-PROTEAN TGX precast gels (Bio-Rad) before transferred to nitrocellulose membranes (Wako). The membranes were incubated in a blocking buffer (Nacalai Tesque) for 1 h at room temperature and then mixed with primary antibodies, including rabbit anti-SARS-CoV-2 Spike (S1/S2) polyclonal antibody (1:2,000; Invitrogen) and mouse anti-β-actin monoclonal antibody (1:5,000; Wako), followed by staining with the horseradish peroxidase (HRP)-conjugated anti-rabbit (1:50,000; GE healthcare) and anti-mouse (1:25,000; GE healthcare) IgG secondary antibodies. The membrane was developed with the ImmunoStar LD enhanced chemiluminescence reagents (Wako) and visualized using ImageQuant LAS 400 (GE Healthcare).

Jurkat reporter cell (JurkatΔ-Luc) for functional analysis of TCRs

DNA fragment of NFAT-RE-Luc2P-SV40 pro-HygroR was amplified from pGL4.3 (Promega) by PCR. The DNA fragment was cloned into Stu I/Sal I site of PiggyBac vector PB530A-2 (SBI) by Gibson assembly method. The resultant vector [PB_NFAT-RE-Luc2P-SV40 pro-HygroR] was electroporated into endogenous TCR knocked-out Jurkat cells[37] with Transposase expression vector PB200PA-1 (SBI). To select Jurkat reporter cell (JurkatΔ-Luc) integrated with NFAT-RE-Luc2P-SV40 pro-HygroR, Hygromycin-B selection was performed at 500 ug/ml concentration for 14 days.

TCR cDNA amplification from single T cells and construction of TCR expression vector

The cryopreserved PBMCs were stained with NF9/A24 and QI9/A24 tetramers, anti-CD8 mAb (RPA-T8; Biolegend), and 7-amino-actinomycin D (7-AAD), and then tetramer^{+}CD8^{+}7-AAD^{-} cells were sorted into 96-well plates (NIPPON Genetics, Cat#

4ti-0770/C) by using an FACS Aria II (BD Biosciences). TCRα and TCRβ cDNA pairs were amplified from single T cells by a one-step multiplex RT-PCR method described in our previous study[19]. The DNA sequences of the PCR products were then analyzed by direct sequencing and the TCR repertoire by IMGT/V-QUEST (https://www.imgt.org/IMGT_vquest/vquest)[38]. The amplified TCRα and TCRβ cDNA fragments were connected to the missing constant region and linked to the blasticidin S resistance (BlaR) gene by the Gibson assembly method with P2A ribosomal skipping sequences. Resultant TCRβ-P2A-TCRα-P2A-BlaR DNA was cloned into the PiggyBac vector (SBI, Cat# PB530A-2) by the Gibson assembly method.

TCR sensitivity assay

The plasmid PB TCR-P2A-BlaR was electroporated into JurkatΔ-Luc with Transposase vector (SBI, Cat# PB200PA-1) using Neon® Transfection System (Thermo Fisher Scientific) under the condition 1200v, 5 ms, 5 pulses. After 48 h, JurkatΔ-Luc cells stably expressing TCRs were selected with RPMI medium containing 10 μg/ml of blasticidin-S for 10-14 days. These cells were cocultured with A549-ACE2-A2402 cells expressing each spike protein an E:T ratio of 2:1 and incubated with RPMI 1640 medium (Thermo Fisher Scientific, Cat# 11875101) containing 10% FBS at 37°C for 6 h. The mixture was measured for luciferase production using a luminescent substrate (Promega, Cat#E2510).

Live virus suppression assay

A549 cells expressing ACE2/A2402 (1×10^4 cells) were infected with each SARS-CoV-2 lineage at an MOI of 0.1 for 120 min at 37 °C. Cells were washed and cocultured with T cells at an E:T ratio of 2:1 and 1:1. Control wells containing virus-infected targets without T cells were also included. After 72 h incubation, culture supernatant was collected and performed real-time RT-PCR. 5 μl of culture supernatant was lysed in an equal amount buffer composed of 2% Triton X-100, 50 mM KCl, 100 mM Tris-HCl (pH 7.4), 40% glycerol and 0.4 U/μl recombinant RNase inhibitor (Promega, Cat# N2615) and then incubated at room temperature for 10 min. 90 μl of RNase-free water (Nacalai tesque, Cat# 06442-95) was added, and 3 μl of diluted sample was used as the template. Real-time RT-PCR analyses for viral RNA copy number was carried out with One Step PrimeScript™ III RT-qPCR Mix (Takara, Cat# RR600B) and reactions were performed by using LightCycler® 96 System (Roche Diagnostics GmbH, Mannheim, Germany). For the primer, Primer/Probe N2 (2019-nCoV) (Takara, Cat# XD0008) were used as follows: NIID_2019-nCOV_N_ forward, 5-AAATTTTGGGGACCAGGAAC-3; NIID_2019-nCOV_N_ reverse, 5-TGGCAGCTGTGTAGGTCAAC-3; and NIID_2019-nCoV_N_ probe, 5-FAM-

ATGTCGCGCATTGGCATGGA-BHQ3. The viral RNA copy number was standardized with a Positive Control RNA Mix (2019-nCoV) (Takara, Cat#XA0142). Relative viral copy was calculated as viral RNA copy number obtained by virus-infected targets without T cells normalized to 1.

QUANTIFICATION AND STATISTICAL ANALYSIS

Data analyses were performed using Prism 9 (GraphPad Software). Data are presented as median or average with SD.

Fig. 1

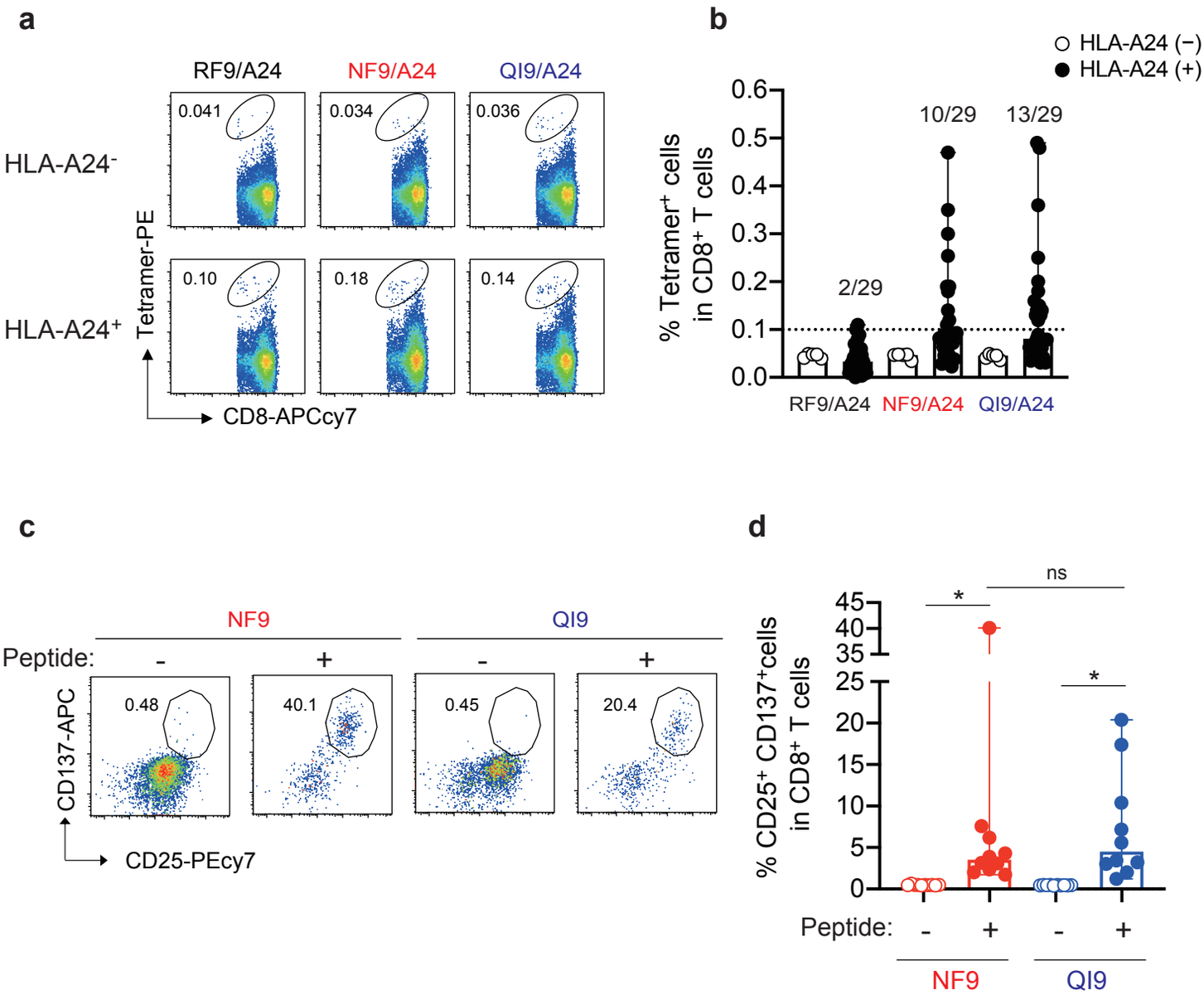

Fig. 2

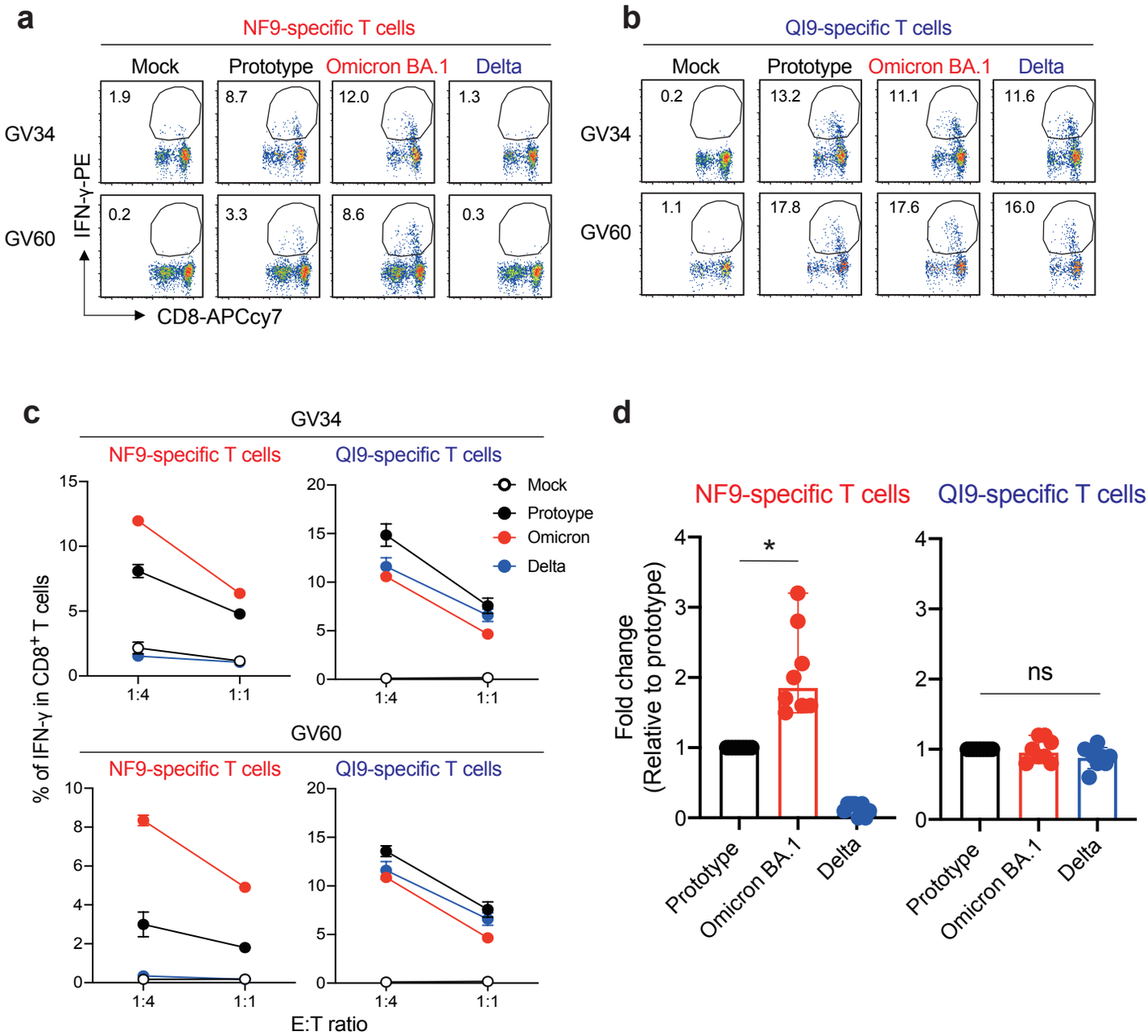

Fig. 3

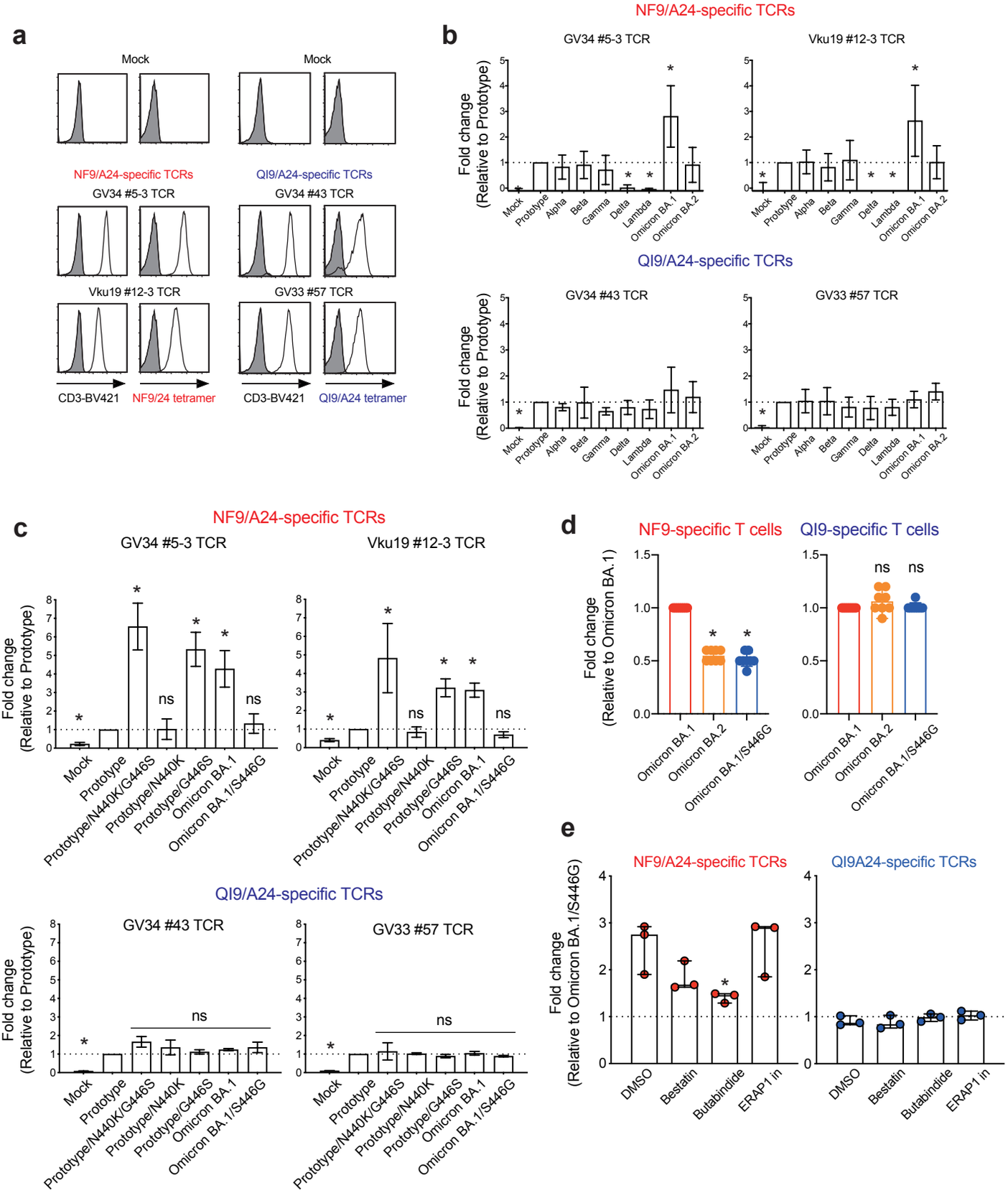

Fig. 4

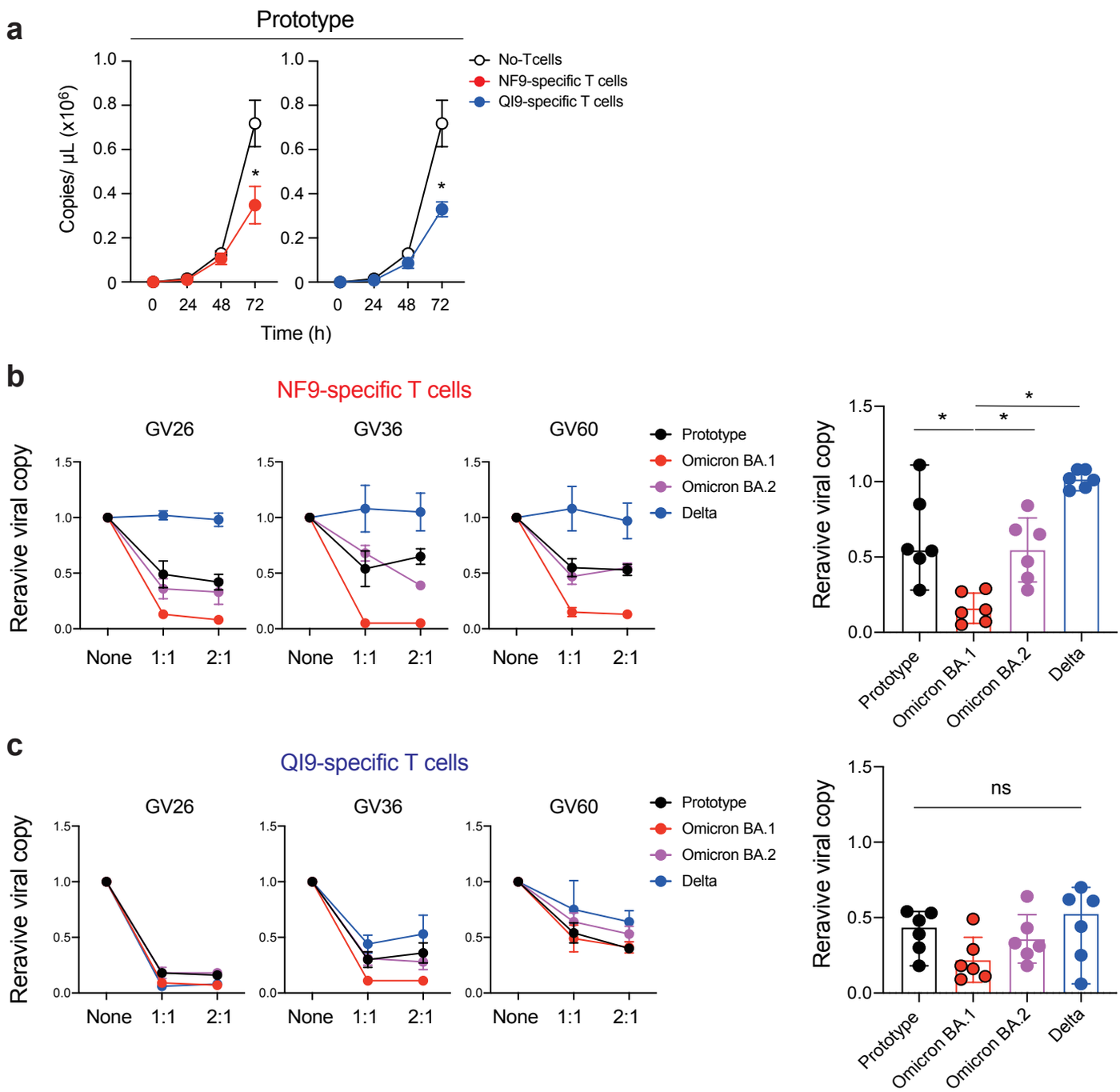

Table 1. Binding of spike-derived epitopes to HLA-A*24:02

Epitope name	Position	Sequence	Normalized Log Kd
RF9/A24	S_{78-86}	RFDNPVLPF	-6.04
NF9/A24	$S_{448-456}$	NYNYLYRLF	-6.89
QI9/A24	$S_{1208-1216}$	QYIKWPWYI	-7.55

Table 2. Spike derived HLA-A24-restricted NF9/A24 epitopes and the N-terminal franking region from the variant

Flanking sequence of the NF9/A24 epitope	Spike mutation	SARS-CoV-2 strain
^{440}NNLDSKV^{446}GG^{448}NYNYLYRLF^{456}	–	Prototype
^{440}K------^{446}S-^{448}---------^{456}	N440K-G446S	Omicron BA.1
^{440}K------^{446}--^{448}---------^{456}	N440K	Omicron BA.2
^{440}-------^{446}--^{448}----R----^{456}	L452R	Delta